

UNCLASSIFIED

AD 407 885

DEFENSE DOCUMENTATION CENTER

FOR

SCIENTIFIC AND TECHNICAL INFORMATION

CAMERON STATION, ALEXANDRIA, VIRGINIA

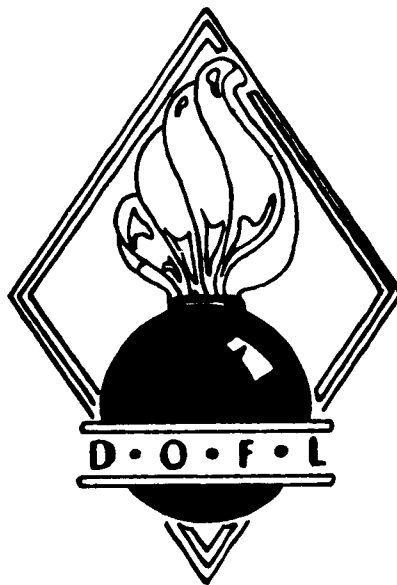


UNCLASSIFIED

NOTICE: When government or other drawings, specifications or other data are used for any purpose other than in connection with a definitely related government procurement operation, the U. S. Government thereby incurs no responsibility, nor any obligation whatsoever; and the fact that the Government may have formulated, furnished, or in any way supplied the said drawings, specifications, or other data is not to be regarded by implication or otherwise as in any manner licensing the holder or any other person or corporation, or conveying any rights or permission to manufacture, use or sell any patented invention that may in any way be related thereto.

**DIAMOND
ORDNANCE
FUZE
LABORATORIES**

407 885



ORDNANCE CORPS

DEPARTMENT OF THE ARMY

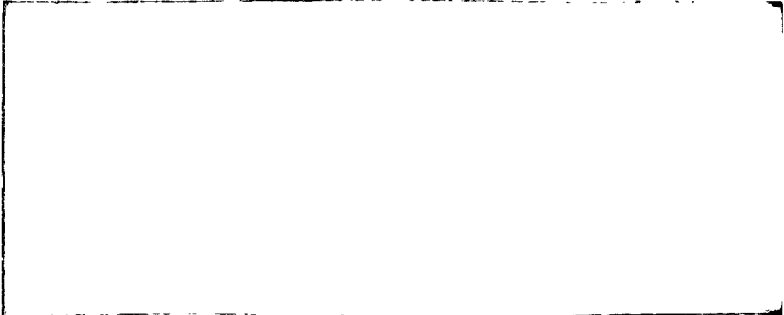
\$4.60

DIAMOND ORDNANCE FUZE LABORATORIES

The Diamond Ordnance Fuze Laboratories, a government research, development, and industrial engineering organization, operates as a component of the Ordnance Corps, Department of the Army. The services and facilities of the Laboratories are available to all of the military services, to Federal scientific agencies, and, in special instances, to non-Government organizations acting privately or as Federal contractors.

The several Laboratories were organized originally to perform the ordnance development activities of the National Bureau of Standards. This work at NBS, under the leadership of Harry Diamond until his death in 1948, resulted in a series of successful proximity fuzes. Among World War II weapon developments, the proximity fuze is considered by many to be second only to the atomic bomb in military importance, and its existence was a closely guarded secret until the end of the war.

Responsibility for proximity fuzing has created a broad technical base, essential to proximity fuze technology, which uniquely prepares DOFL to participate in a wide variety of seemingly unrelated scientific and technical activities.



DOFL has a creative force of scientists, engineers, skilled craftsmen, and supporting personnel numbering almost 1400. Its staff integrates both government and industrial backgrounds. Invaluable experience is constantly being acquired as a result of extensive in-house research and development work. DOFL has frequently worked in close cooperation with other government agencies, and with industrial and educational institutions in carrying out research, development, and production engineering. DOFL is thoroughly qualified to understand, collaborate with, and supervise industrial contractors in many specialized areas. The common denominator of DOFL's wealth of specialized knowledge and wide experience is creative thinking -- and the ability to rapidly translate this into hardware of landmark quality. Advanced ideas and inventive thinking are specifically oriented toward the needs of the ultimate user.

DOFL's technical competence is exemplified by new things. Its personnel often establish new trends in electronic and mechanical design. Ammunition concepts in electronic packaging, printed circuits, microminiaturization, casting resins, flow and temperature measurement systems, high-resolution radar, air navigation systems, reserve power supplies, telemetering equipment, nuclear effects studies, and the revolutionary fluid amplifier are all major areas where DOFL productivity has made significant contributions to the National capability. Each of these contributions has both military and civilian value. The abilities supporting such accomplishments provide the Diamond Ordnance Fuze Laboratories with unique potential for further progress.

DDC
RECEIVED
JUN 20 1963
TISIA D

ABSTRACT

This ^{report} ~~proposal~~ describes a recommended program of laboratory study of environmental conditions around hypersonic missiles.

The study of the properties of plasmas has been carried on to date using noble gases and will be extended to oxygen-nitrogen mixtures. Three diagnostic techniques capable of being used simultaneously are ~~as follows:~~

- 1) Measurements made by propagating 10 kmc across the plasmas behind the shockwave.
2. Measurements made of the radiated power at 10 kmc emitted by the hot gas.
3. Measurements made of the Stark broadening of certain spectral lines.

These methods will yield information on the degree and rates of ionization, electron density, electron temperature, collision cross-section, attenuation and phase velocity constants, and reflection coefficient. This information will provide an understanding of mechanism of attenuation of radio signals through the plasma and will lead to approaches for solution of this problem.

1. SCOPE

General Objectives

This program is concerned with the laboratory study of environmental conditions to be found around hypersonic missiles. The shock tube program thus encompasses the investigation of the physical, chemical, and electromagnetic properties of high temperature gas created by a one-dimensional shock. Initial studies have commenced with noble gases and will be extended to oxygen-nitrogen mixtures both with and without applied magnetic fields.

The first parameter to be determined will be electron density. Measurements will be obtained simultaneously from the microwave experiment, from observation of Stark line broadening and from conductivity measurements.¹ This experiment will serve to calibrate the microwave equipment and to correlate the various experimental techniques. Identical techniques will then be employed in later experiments as diagnostic tools.

1. Lin, S.C., E. L. Resler, and A. Kantrowitz, Electrical Conductivity of Highly Ionized Argon Produced by Shock Waves, J. A. P., 1, 95, Jan '55

2. MICROWAVE PROPAGATION EXPERIMENT

A. Objectives

The microwave propagation experiment can be treated as a distinct entity with its own research objectives. These are:

(1) Evaluation of the proposed technique as a more precise method for determining electron density in shock tube experiments.

(2) Measurement of electromagnetic properties of ionized gases using single particle theory and determination of the limitations of this theory.

(3) Use of the developed techniques as a diagnostic tool for plasma analysis as a function of various gas parameters.

(4) Extension of the experiments to include plasma studies with an applied magnetic field.

B. Planned Approach

The first plasma to be studied will be formed by a shock wave in argon. The ionized gas (assumed uniform) will be passed through one branch of a microwave bridge circuit where it will affect the propagation of a 10 kmc signal. Comparison of this signal with a reference signal will yield information on electron density, collision cross-sections, attenuation and phase velocity constants, and reflection coefficient. The theory of these measurements is given in section III A.

The equipment will be calibrated by comparison of the measured results with simultaneous measurements determined from Stark line broadening using time resolved spectrographic equipment, and by conductivity measurements using the method of Lin et al.² The measurements will be made for a range of electron densities of 10^{10} - 10^{13} elecs/cm³ and for gas pressures of approximately 1 - 100 cm Hg.

2. See reference 1.

The knife edged section is aligned with the flow streamlines so as to introduce negligible disturbance to the gas flowing into the waveguide. The microwave ceramic windows (brazed into the waveguide) are reflectionless (one-half wavelength) at the test frequency and comprise a continuation of the knife edge walls so as to maintain streamline flow. The microwave signal is transmitted through the plasma (transverse to plasma flow) by the waveguides. An assembled view of the parts is shown in figure 2. The section is shown in the shock tube

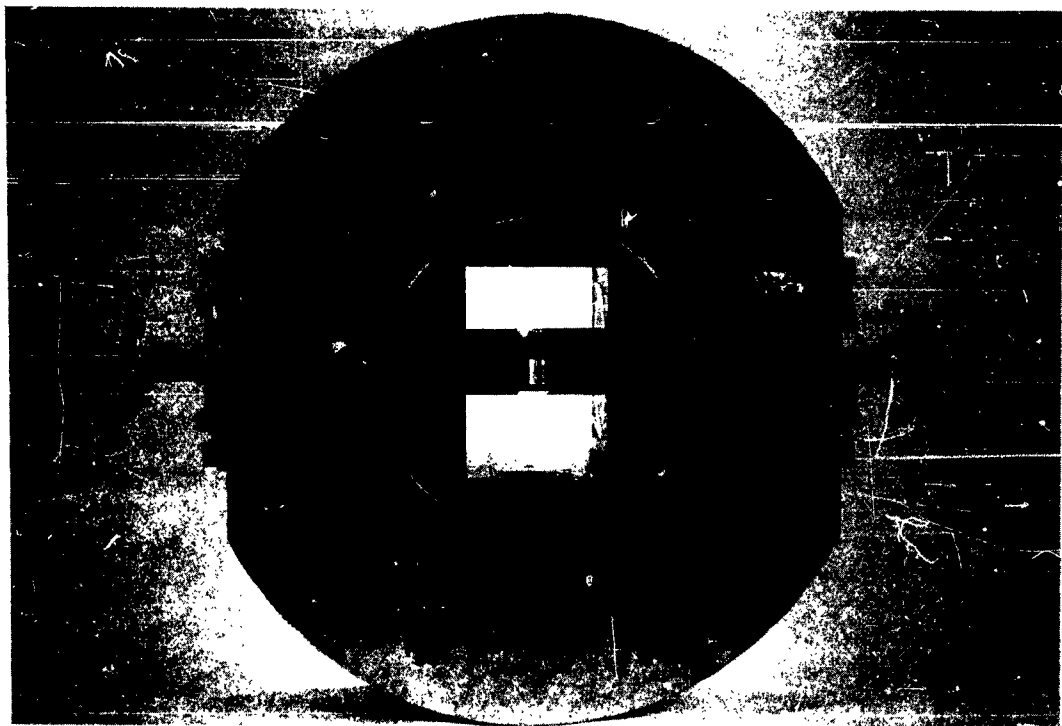


Figure 2. Assembled view of the shock tube microwave test section.

together with the bridge portion of the microwave circuit in figure 3. An overall view of the test bench is shown in figure 4.

In figure 3, a signal of known frequency and power is fed into a 3db power divider which feeds the two branches of the bridge circuit. Attenuators and a line stretcher permit balancing of the branches when the test section is filled with inert gas. The output of the two branches



Figure 3. Microwave bridge circuit in the shock tube.

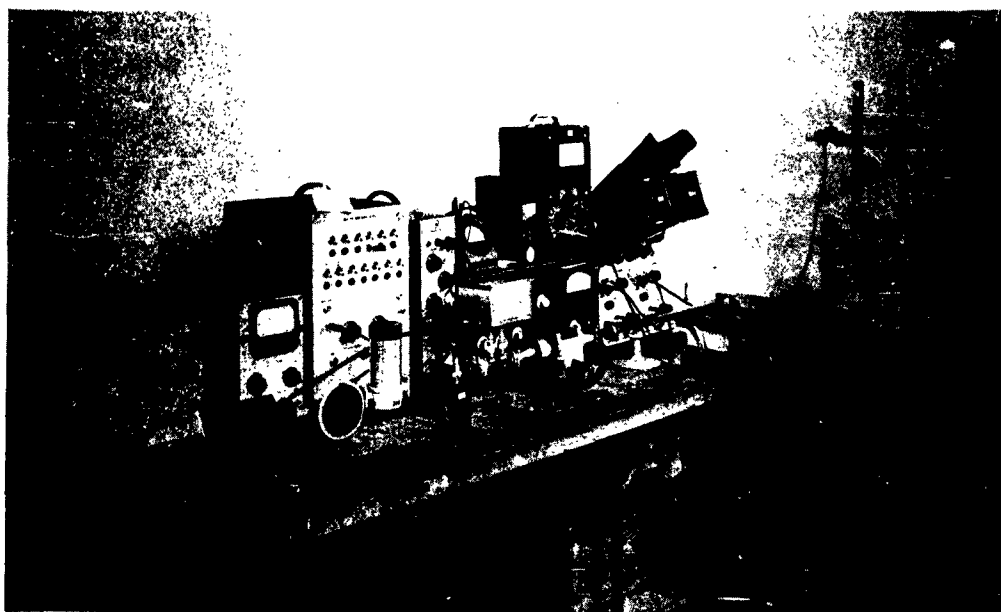


Figure 4. Overall view of microwave test bench.

feed a magic T whose output arms, terminated with crystals, feed a dual beam oscilloscope for time resolved measurements. The two crystal outputs are (a) the vector sum of the test and reference signals and (b) the vector difference of the two signals. The amplitude and phase of the test signal will be determined by the properties of the plasma. Simultaneous analysis of the two recorded signals yields plasma parameters as a function of time. The theory of the measurements is given in section III A.

III. Theory of Measurements

A. Microwave Propagation Experiments

The dielectric properties of a material can be completely described by specifying the complex permittivity constant

$$\epsilon_r^* = \epsilon_r' - j\epsilon_r'' \quad (1)$$

which is defined by the relation

$$\vec{J}_T = j\omega\epsilon_0\epsilon_r^*\vec{E} = \vec{J}_c + \epsilon_0\frac{\partial\vec{E}}{\partial t} \quad (2)$$

where \vec{J}_c = conductor current

\vec{J}_T = total current

ϵ_0 is free space permittivity

j is $\sqrt{-1}$

\vec{E} is the electric field vector of the form

$\vec{E}_0 e^{j\omega t}$ where t is time and ω is radian

electromagnetic frequency

An electron in this field will oscillate 90° out of phase with \vec{E} with its velocity \vec{v} given by

$$\vec{V} = \frac{e}{m} \left(\frac{1}{\nu + j\omega} \right) \vec{E} \quad (3)$$

where e is electron charge and m is its mass; ν is a constant defined as the collision frequency and is related to collision losses. By writing

$$\vec{J}_c = Ne\vec{V} \quad (4)$$

where N is the electron density; and substituting into

$$\vec{J}_t = \vec{J}_c + \epsilon_0 \frac{\partial \vec{E}}{\partial t} \quad (5)$$

then comparing with equation 2 we get a relation between

$$\epsilon_r', \epsilon_r'', \nu, \text{ and } \omega_p$$

where plasma frequency $= \omega_p$

$$\omega_p = \sqrt{\frac{Ne^2}{m\epsilon_0}} \quad (6)$$

$$1 - \epsilon_r' = \frac{\omega_p^2}{\nu^2 + \omega^2} \quad (7)$$

$$\epsilon_r'' = \frac{\omega_p^2}{\nu^2 + \omega^2} \cdot \frac{\nu}{\omega} \quad (8)$$

For a TE wave, traveling in the z direction and polarized in the y direction,

$$\vec{E}_y = \vec{E}_o e^{j\omega t - \gamma z} \quad (9)$$

$$\gamma = \alpha + j\beta \quad (10)$$

Where γ is the propagation constant, α the attenuation constant, and β the phase velocity constant, it can be shown that ϵ_r' and ϵ_r'' are related to α and β (for the dielectric filled waveguide) and the free space and guide wavelengths in the following form³:

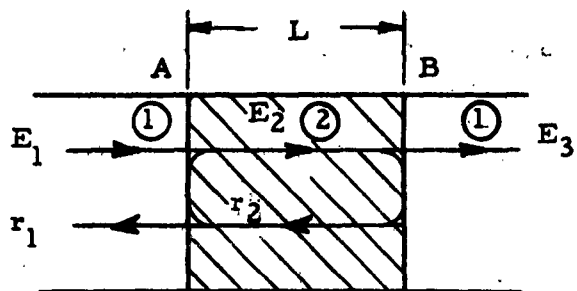
$$(1 - \epsilon_r') = \left(\frac{\lambda_o}{\lambda_g} \right)^2 \left[1 + \left(\frac{\alpha_\epsilon}{\beta_o} \right)^2 - \left(\frac{\beta_\epsilon}{\beta_o} \right)^2 \right] \quad (11)$$

$$\epsilon_r'' = 2 \left(\frac{\lambda_o}{\lambda_g} \right)^2 \left[\left(\frac{\alpha_\epsilon}{\beta_o} \right) \left(\frac{\beta_\epsilon}{\beta_o} \right) \right] \quad (12)$$

where subscripts ϵ refer to dielectric filled guide, subscript o refers to air filled waveguide, λ_o is free space wavelength, λ_g is wavelength for air filled guide.

-
3. Tischer, F. J., Measurement of the Wave Propagation Properties of Plasma in the Microwave Region, Ohio State Univ. Rpt 941-1 20 Aug '59, Diamond Ordnance Fuze Laboratories, Ordnance Corps Contract DA-49-186-502-)RD-816, 17 pp.

For the dielectric slab approximation, we take into account reflections at surfaces A and B



Scattering Diagram (Region 1 air, region 2 dielectric)

where ρ , the reflection coefficient can be written in terms of β_o and λ_ϵ as

$$\rho_{12} = \frac{j\beta_o - \gamma_\epsilon}{j\beta_o + \gamma_\epsilon} \quad (13)$$

and defining a complex transmission coefficient

$$\tau^* = \frac{\vec{E}_3}{\vec{E}_1} \quad (14)$$

we find that

$$\frac{1}{\tau^*} = \frac{1}{2} \left(\frac{\gamma_\epsilon L}{j\beta_o L} + \frac{j\beta_o L}{\gamma_\epsilon L} \right) \sinh \gamma_\epsilon L + \cosh \gamma_\epsilon L \quad (15)$$

The magnitude of τ can be found from the relation

$$|\tau| = \frac{|E_3|}{|E_1|} \quad (16)$$

The $\underline{\tau}$ can be determined by measuring the change in angle $\Delta\phi$ for the plug section when air filled and dielectric filled, and then invoking the relation

$$\underline{\tau} = \Delta\phi + \beta_0 L \quad (17)$$

For static measurements a bridge circuit as shown in figure 5 may be used.

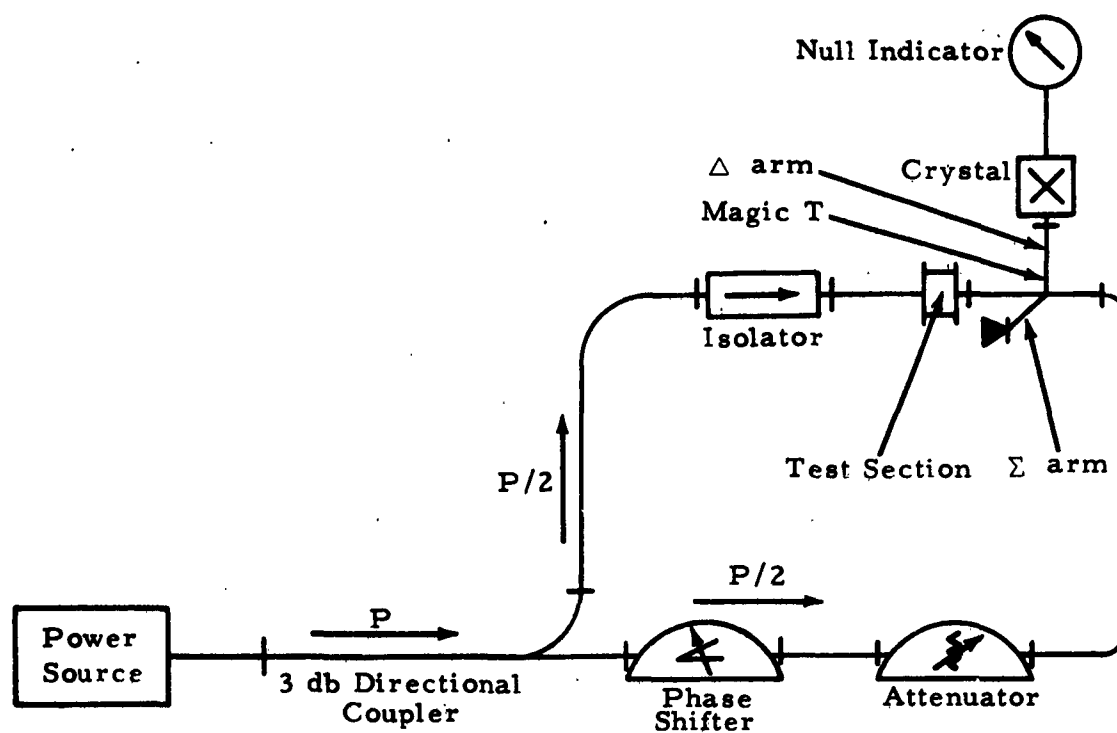


Figure 5. Microwave bridge circuit (steady state).

The precision attenuator and phase shifter are adjusted for a minimum output and these readings correlated with $\underline{\tau}$ and τ by

$$20 \text{ Log } \tau_{\epsilon}^{-1} = A^{\text{db}} = \text{attenuation reading} \quad (18)$$

$$\underline{\angle \tau} = \Delta \phi + \beta_0 L \quad (19)$$

$\Delta \phi$ is the phase shifter reading of the angle difference.

For dynamic measurements a similar circuit, figure 6 is used but instead of balancing, a magic T is employed to yield the vector sum E_Σ and the vector difference E_Δ of the reference signal E_R and the test signal E_T , Figure 7.

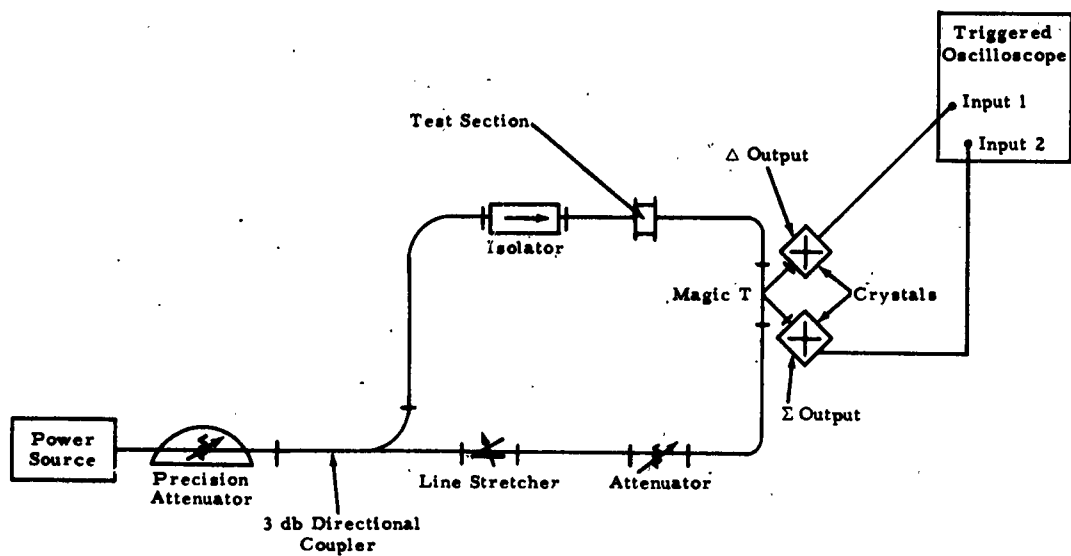
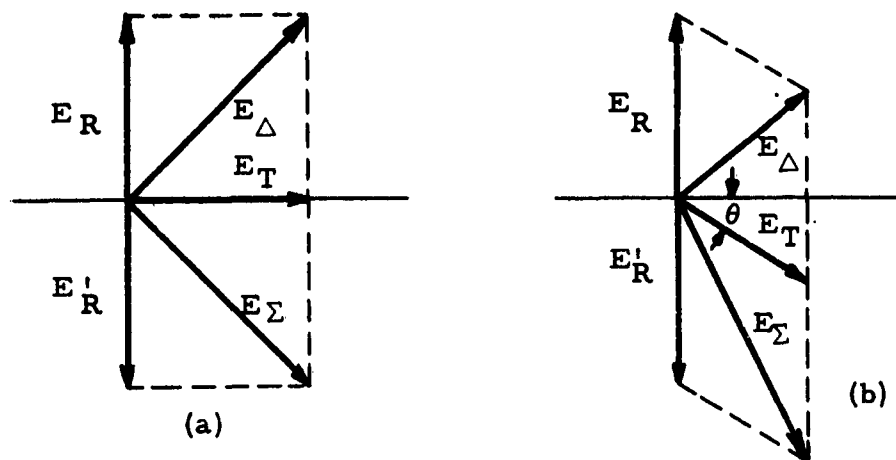


Figure 6. Microwave bridge circuit (transient measurement).



$$E_T = \left[\frac{E_\Sigma^2 + E_\Delta^2}{2} - E_R^2 \right]^{1/2}$$

$$\theta = \sin^{-1} \frac{E_\Sigma^2 - E_\Delta^2}{4 E_T E_R}$$

Figure 7. Voltage relations in the complex plane.

Two time resolved outputs are obtained, from which $|\tau|$ and $\angle\tau$ can be obtained from the relations

$$|\tau| = \frac{|E_3|}{|E_1|} = \left[\frac{E_\Sigma^2 + E_\Delta^2 - 2E_R^2}{2E_R^2} \right]^{1/2} \quad (20)$$

$$\frac{\angle \tau}{\beta_0 L} = \sin^{-1} \frac{E_{\Sigma}^2 - E_{\Delta}^2}{4E_T E_R} \quad (21)$$

C. Shock Tube

The shock tube is a device for the production of transient high temperature gas. A high pressure section is separated from a low pressure section by a scored diaphragm. The gas pressure in the high pressure section is increased until the diaphragm is made to burst. A shock wave is formed and propagates into the low pressure gas, which is initially at equilibrium. The disturbance compresses the gas, raises its temperature and for shocks in argon greater than Mach 6, results in sufficient ionization to affect x-band propagation. The equilibrium degree of ionization behind the shock front can be calculated.^{1, 2}

IV. Achievements to Date³

Preliminary measurement of a helium shot into argon has been made. A typical oscillograph for a Mach 8 shock into argon, initially at a pressure of 1 cm Hg, is shown in Figure 8. The upper curve is the vector difference of the test signal and reference signal; the lower curve is the vector sum of the two signals. Time is from left to right. The two time bases are correlated accurately by using a time mark generator to form the 10 μ secs blanking marks. The scope is triggered 150 μ secs before the shock reaches the test section. The deflections before and after the main transient pulse are 3db calibration marks.

1. Petschek, H. and S. Byron, Approach to Equilibrium Ionization Behind Strong Shock Waves in Argon, *Annals of Physics*, 1, 270, 1957
2. Bond, J.W. Jr., Structure of a Shock Front in Argon, *Phys. Rev.* No. 105, 1683 - 15 March '57
3. F. L. Tevelow and H. D. Curchack, Shock Tube-Microwave Propagation measurements using the dielectric slab approximation. To be presented 2nd MHD Symposium, Phila, Pa., March 9, 10, 1961.

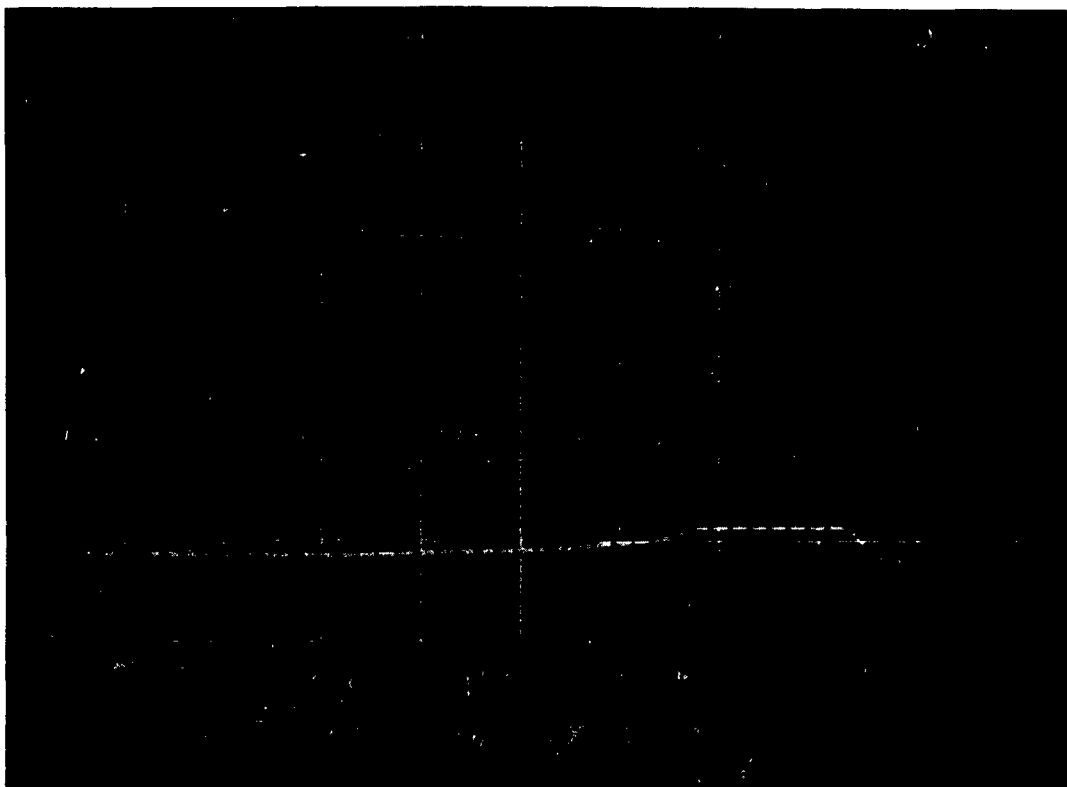


Figure 8. Results of microwave propagation through a plasmas formed by a Mach 8 shock in argon (upper curve is the vector difference of the test signal and a reference signal. Lower curve is the vector sum of the two signals.)

Deflections as a function of time are measured, compared with calibration curves for the crystals, and the resultant voltages fed into a computer program. The results of a computer run are shown in figure 9. Computed values are τ , ϵ_r' , ϵ_r'' , α , β , ν , ω_p , N and the complex reflection coefficient. Figure 10 shows computed values of electron density for three shots at 1 cm Hg and Mach 8. Figure 11 shows computed values of collision frequency. Precision of the computed value of electron density is estimated at 25%, that of collision frequency as good as 50%. Relative measurements are expected to be much better than this.

The following figures are pertinent to section 3 of this proposal.

Fig. 12. Equipment arrangement. A drum camera and a spectrograph are used to analyze the light emitted from a quartz window in the shock tube.

SHOT NUMBER 406											
BETA 0 2 L = 1.0000000E 00 LAMBDA SQUARE = 5.6232999E-01 OMEGA = 6.2831852E 10 TIME SIG/DEL ABSTAU SIN(PHI) GAMMA EPSILON NU P OMEGA P N RHO RHOIN EXP R											
0	0.707	1.00	0.	3.022E-04	1.000E 00	0.	0.	0.	-4.098E-08	-1.374E-04	2.2E-08 2.37E-1
30	0.709	1.00	0.00	-2.527E-03	9.968E-01	-5.617E 10	4.775E 09	7.167E 09	1.510E-03	3.154E-03	7.3E-08 7.7E-1
50	0.713	1.01	0.01	-8.184E-03	9.904E-01	-6.070E 10	8.543E 09	2.295E 10	4.202E-03	9.757E-03	1.3E-08 1.7E-1
80	0.716	0.99	0.03	5.688E-03	9.648E-01	1.075E 10	1.199E 10	4.519E 10	1.602E-02	1.909E-02	1.3E-08 1.7E-1
7.6 X 10 ⁻²	0.694			9.684E-01	6.052E-03				2.833E-03	1.863E-02	
7.1 X 10 ⁻¹	0.719	0.99	0.04	5.137E-03	9.551E-01	7.853E 09	1.342E 10	5.681E 10	2.053E-02	2.499E-02	0. 4.2 X 10 ⁻⁴
	0.691			9.598E-01	5.614E-03				2.675E-03	2.266E-02	
1.1 X 10 ⁻¹	0.722	0.99	0.05	8.857E-03	9.409E-01	1.009E 10	1.552E 10	7.568E 10	2.752E-02	3.174E-02	1.3E-08 1.7E-1
	0.683			9.464E-01	9.546E-03				4.676E-03	3.175E-02	
2.0 X 10 ⁻¹	0.727	0.98	0.07	1.479E-02	9.162E-01	1.166E 10	1.850E 10	1.075E 11	3.944E-02	4.276E-02	0. 1.6 X 10 ⁻³
	0.675			9.236E-01	1.555E-02				7.991E-03	4.707E-02	
1.8 X 10 ⁻¹	0.732	0.98	0.09	1.341E-02	9.006E-01	8.771E 09	2.000E 10	1.258E 11	4.783E-02	5.236E-02	0. 7.5 X 10 ⁻³
	0.670			9.086E-01	1.388E-02				7.363E-03	5.415E-02	
3.3 X 10 ⁻¹	0.735	0.97	0.11	2.352E-02	8.771E-01	1.214E 10	2.243E 10	1.581E 11	6.035E-02	5.978E-02	7.3E-08 3.4 X 10 ⁻³
	0.659			8.859E-01	2.373E-02				1.323E-02	7.201E-02	
3.2 X 10 ⁻¹	0.746	0.97	0.14	2.278E-02	8.537E-01	8.509E 09	2.553E 10	2.068E 11	8.322E-02	6.089E-02	2.3E-08 5.4 X 10 ⁻³
	0.645			8.461E-01	2.195E-02				1.537E-02	9.543E-02	
5.2 X 10 ⁻¹	0.751	0.96	0.18	3.792E-02	7.986E-01	1.084E 10	2.862E 10	2.574E 11	1.077E-01	9.165E-02	0. 1.1 X 10 ⁻²
	0.627			8.048E-01	3.475E-02				2.327E-02	1.234E-01	
7.6 X 10 ⁻¹	0.759	0.94	0.23	5.693E-02	7.436E-01	1.139E 10	3.234E 10	3.287E 11	1.560E-01	1.068E-01	2.1E-08 7.7E-1
	0.603			7.834E-01	4.650E-02				3.611E-02	1.637E-01	
11.1 X 10 ⁻¹	0.764	0.91	0.27	8.091E-02	6.880E-01	1.256E 10	3.579E 10	4.027E 11	1.897E-01	1.149E-01	2.0E-08 3.5 X 10 ⁻¹
	0.578			6.771E-01	6.239E-02				5.740E-02	2.088E-01	
21.0 X 10 ⁻¹	0.765	0.90	0.29	9.477E-02	6.659E-01	1.319E 10	3.711E 10	4.328E 11	2.083E-01	1.159E-01	1.3E-08 7.37E-1
	0.568			6.498E-01	7.013E-02				6.941E-02	2.243E-01	
15 X 10 ⁻¹	0.768	0.89	0.32	1.108E-01	6.333E-01	1.311E 10	3.887E 10	4.749E 11	2.388E-01	1.194E-01	1.3E-08 5.6 X 10 ⁻¹
	0.554			6.068E-01	7.655E-02				8.541E-02	2.488E-01	
16 X 10 ⁻¹	0.768	0.89	0.32	1.164E-01	6.266E-01	1.354E 10	3.925E 10	4.842E 11	2.449E-01	1.191E-01	1.3E-08 6.0 X 10 ⁻¹
	0.551			5.981E-01	7.928E-02				9.066E-02	2.541E-01	
21.7 X 10 ⁻¹	0.768	0.86	0.36	1.581E-01	5.807E-01	1.449E 10	4.175E 10	5.479E 11	2.874E-01	1.155E-01	3.2E-08 7.8 X 10 ⁻¹
	0.531			5.372E-01	9.659E-02				1.324E-01	2.896E-01	
27.7 X 10 ⁻¹	0.768	0.84	0.39	2.011E-01	5.397E-01	1.506E 10	4.386E 10	6.039E 11	3.254E-01	1.113E-01	1.3E-08
	0.514			4.817E-01	1.105E-01				1.199E-01	3.195E-01	1.3 X 10 ⁻¹
33.2 X 10 ⁻¹	0.767	0.82	0.41	2.409E-01	5.098E-01	1.561E 10	4.533E 10	6.458E 11	3.476E-01	1.059E-01	0. 17

Figure 9. Computer data reduction for shot number 406 shown in Figure 8.

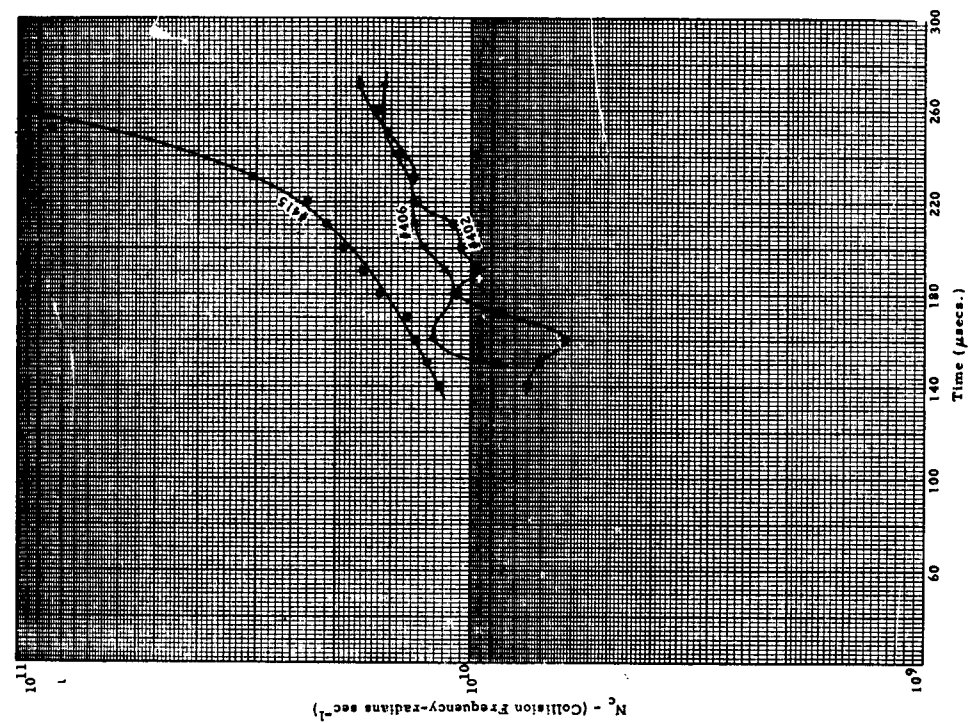


Figure 10. Electron density behind a Mach 8 shock in argon.
(High impurity level #415. $p = 10\text{cm Octoil}$)

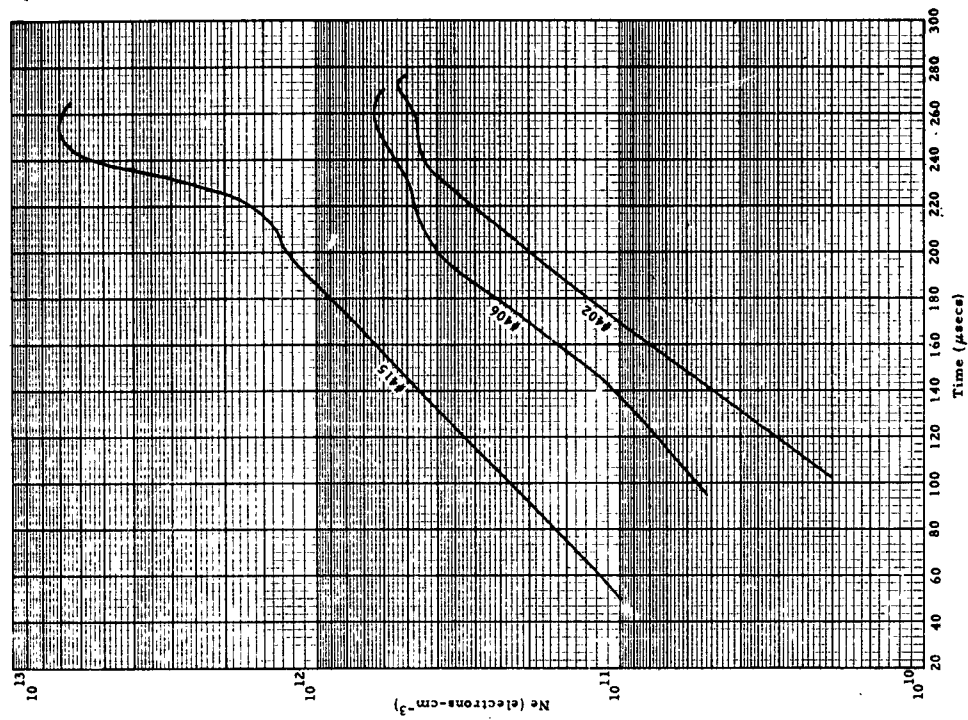


Figure 11. Collision frequency behind a Mach 8 shock in argon.
(#415 is a high impurity level shot. $p = 10\text{cm Octoil}$)

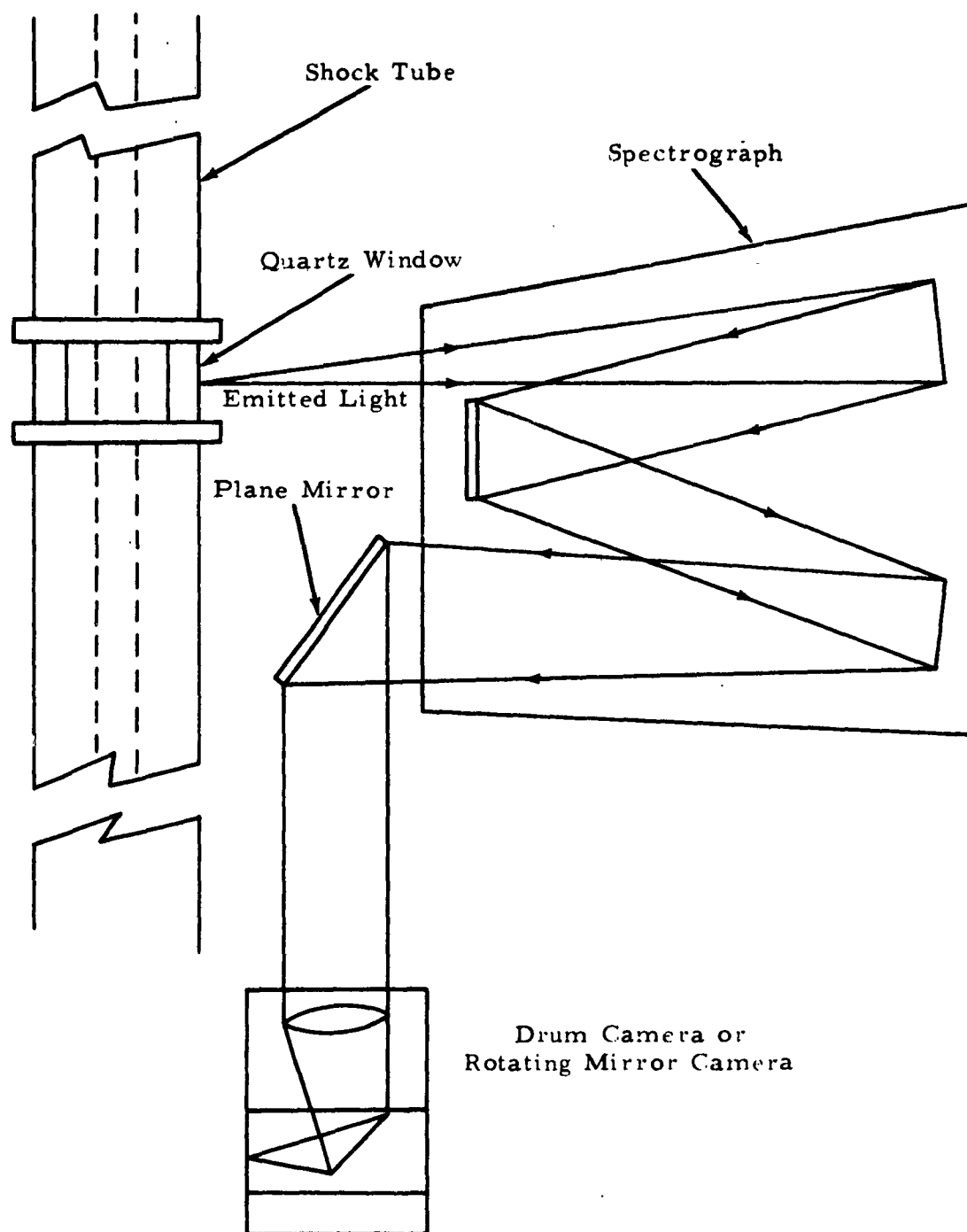


Figure 12. Equipment arrangement.

3. STARK LINE BROADENING

V. Discussion of Theory:

Of much concern to the theoretical physicist and of fundamental importance to any understanding of physical processes especially those involving many-body collisions, is the manner or "mechanism" whereby energy is transferred from one degree of freedom to another. In particular, there is interest in the mechanism whereby a gas, initially having all its energy in the kinetic mode, distributes the energy to the other possible modes such as excited states and ionization of the atoms. The distribution of this energy finally results in an equilibrium condition wherein each degree of freedom has the same average energy.

The process whereby energy is distributed among the various degrees of freedom is called equilibration. The classical description of equilibration assumes that collisions between atoms or molecules cause the transfer of energy between them with the result that the atoms and molecules are dissociated, excited and ionized. (It is assumed that enough energy is available for this process.)

If the classical assumptions of collisions provide a reasonable description of the behavior of gases, then a classical analysis using concepts of cross-section, inelastic collisions, two-body collisions, etc., predicts that there exists a fairly well defined rate of equilibration. To date there has been a discrepancy between the experimentally determined rate and the calculated rate of equilibration. (1), (2) and (3).

(1) J. W. Bond, Phys. Rev. 105, 1683 (1957)

(2) H. Petschek and S. Byron, Annals of Physics 1, 270 (1957)

(3) H. D. Weymann, University of Maryland TNBN-144,

AFOSRTN 58-788, July 1958

The technique of measurement proposed here is based upon the effect of strong electric fields on the radiation emitted by excited atoms. When atom-atom collisions are sufficiently energetic, atoms become excited and ionized. The presence of ions and free electrons causes strong local electric fields in the vicinity of the excited atoms causing perturbations in the emitted radiation. This effect of an electric field on radiation is called the Stark effect and consists essentially in a shift and broadening of the possible frequencies emitted by the atom.

The amount of broadening of a given line is proportional to the strength of the electric field which in a high temperature gas is proportional to the concentration of ions and electrons in the gas. As a consequence, a study of the emitted light will give a direct measurement of the degree of ionization rates.

The light emitted must be studied spectroscopically to obtain a time resolved plot of the width ($\Delta\lambda$) of a line in the spectrum of high temperature gas. The amount of line broadening due to free electrons and ions has been recently calculated using the theory to a moderately high precision by Kolb, Griem and Shen for the Balmer series of hydrogen.⁽⁴⁾ More recently the lines of neutral and singly ionized helium have been calculated. Using these calculations, a determination can be made of the rate at which ions and electrons are produced. This is the rate for the whole equilibration process.

(4) A. C. Kolb and H. Griem, Phys. Rev. 111, 514, C 1958
Phys. Rev. 116, 4 (1959) Naval Research Lab Report 5455,
4 March 1960

VI. Description of Experimental Techniques and Equipment Available

The essential elements of the equipment for this experiment are (1) a shock tube, (2) a spectrograph, (3) a high speed camera and (4) a microdensitometer. Equipment arrangement is in Figure 12.

The shock tube to be used in the initial series of experiments is a gas driven, heated driver shock tube having a 2" x 2" square cross section. This shock tube was designed and built at DOFL and has been in use for several years. The test section is approximately seventeen feet long. At present there are observation ports for use of interferometric, spectrographic and microwave equipment. With this shock tube, using the heated driver, it is possible to obtain shock waves in a gas having Mach numbers greater than 13. At these Mach numbers the shock heated gas is quite luminescent and the ion density is about 10^{17} electrons per cubic centimeter, depending upon the initial gas pressure in the test section.

The spectrograph to be used in this experiment is a Jarrell-Ash Model 75-000, a plane grating spectrograph of large aperture (F/6.3) and relatively high resolution (.4A/mm). The use of this type of spectrograph is demanded by the short time duration of the experiments.

To obtain time resolution of the emitted light, the light dispersed by the spectrograph is allowed to fall on the film of a high speed camera. Two cameras are available for this purpose. One camera is a high speed drum camera of DOFL design, capable of film speeds of 500 ft/sec. which is equivalent to a time resolution of the order of 5 microseconds. The other camera is a rotating mirror type, a Beckman-Whitley Model 194 streak camera. The latter camera is capable of time resolution of the order 0.5 microseconds.

The remaining essential items of equipment is a microdensitometer. The one to be used is a console recording type designed and built by Jarrell-Ash. It is now used at the University of Maryland by Dr. Hans Griem and his research group.

The procedure for the experiment follows. The shock tube is pumped down to a pressure of about 10^{-6} mm of Hg to insure low concentration of impurities. An amount of pure argon gas is allowed to

flow into the tube until the desired initial pressure is obtained (1 cm Hg). The pressure in the driver section is then built up until the metal diaphragm separating the two sections of the shock tube breaks, allowing the high pressure gas to expand and cause a shock wave in the argon test gas. The velocity of the shock is recorded by six pressure pickups mounted in the tube.

The shock-wave acts on the gas, heating it to such an extent that it becomes luminescent. The light emitted passes through a quartz window to the entrance slit of the spectrograph. Of the lines emitted by the gas, several are chosen to be recorded and analyzed. These lines are the Balmer lines of hydrogen or the neutral lines of helium. (Helium or hydrogen will be present in the test gas as an impurity of less than 0.01%). This impurity level is not expected to be high enough to affect the study of argon but will be sufficient to be used as an indicator for the analysis. The lines selected to be studied are focused on the film of the camera. A typical trace is as in figure 13.

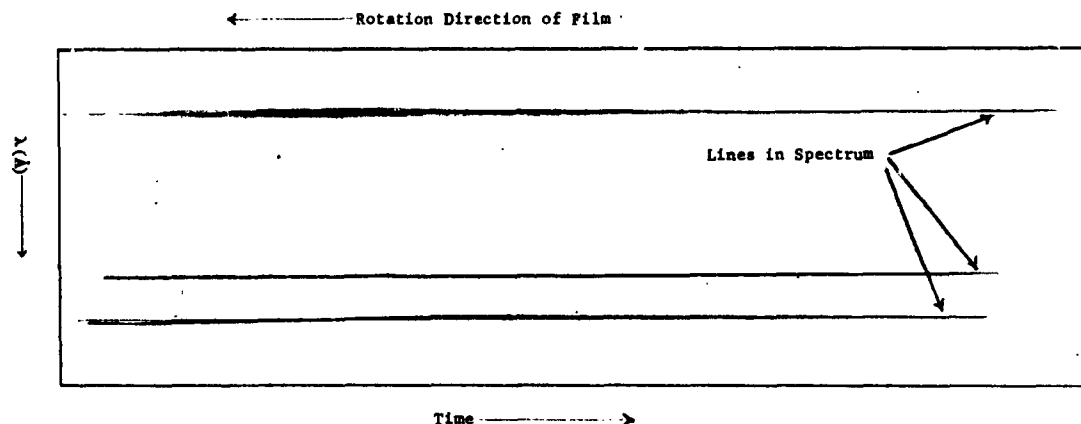


Figure 13. A typical film exposure from camera. Notice that lines vary in intensity and width as a function of time.

A line is chosen to be analyzed. The width of the line and its position is plotted for various times. A plot obtained for a typical time appears as in figure 14. This curve is related to the calculations of Kolb, Griem and Shen to obtain the electron density causing this particular profile. Since profiles are obtained for various times behind the shock front, we obtain electron density versus time behind the shock, the desired information.

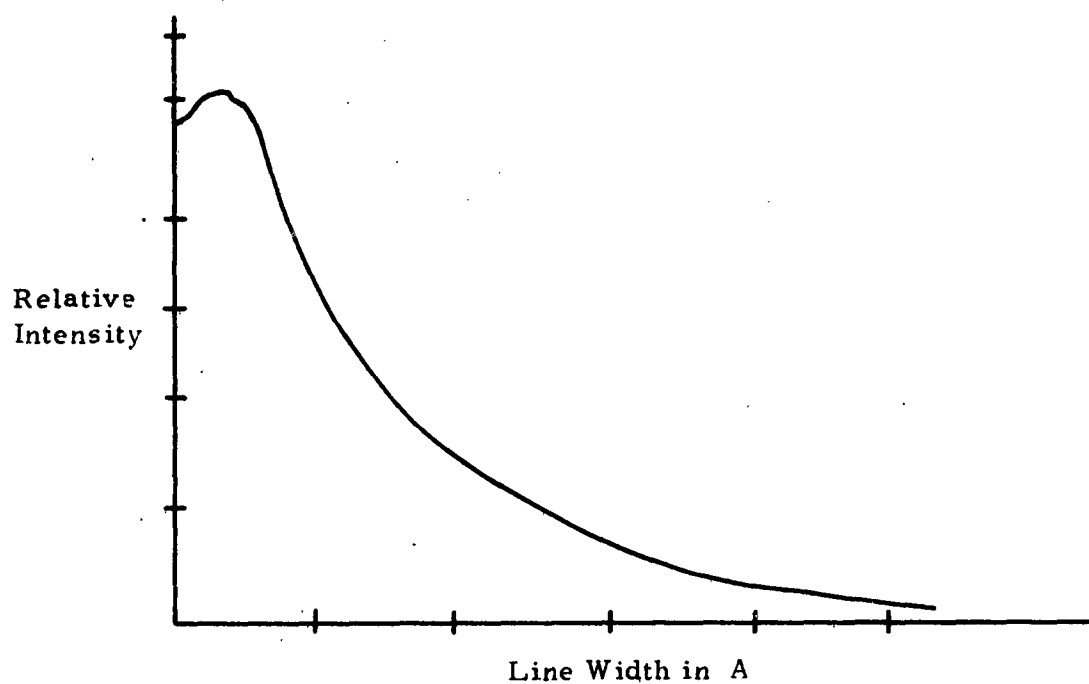


Figure 14. A curve of intensity versus wavelength for a given line at a given time behind the shock.

4. ELECTRON TEMPERATURE MEASUREMENTS BY EMITTED MICROWAVE RADIATION

VII. Discussion

A black body emits radiation at all frequencies in accordance with the formula

$$\psi_{\lambda} = \frac{8\pi ch}{\lambda^5 \left(e^{\frac{ch}{\lambda kT}} - 1 \right)}$$

where ψ_{λ} is the energy density of radiation inside an equivalent isothermal enclosure, h is Planck's constant, c is the velocity of light, k is Boltzmann's constant, λ is the wavelength and T is the temperature of the black body in $^{\circ}\text{K}$.

This equation gives the energy density of the black body as a function of frequency and temperature. If this equation is plotted it will be observed that as the body temperature increases the density of radiation at all frequencies increases and that, the peak of the energy density curve is displaced toward the higher frequencies.

The wavelength, λ_m at which the energy density is a maximum was first expressed quantitatively by Wien in the following equation

$$\lambda_m T = 0.294 \text{ cm degree}$$

Although the radiation density is highest in the optical region there is nevertheless, an appreciable amount of radiation at the lower frequency segment of the spectrum. We are interested in the radiation at these lower frequencies.

For this application, some simplification of Planck's law may be made. Expanding $e^{\frac{ch}{\lambda kT}}$ in a series,

$$\psi_{\lambda} = \frac{8\pi ch}{\lambda^5} \left[\frac{1}{\left(\frac{ch}{\lambda k}\right)\left(\frac{1}{T}\right) + \frac{1}{2} \left(\frac{ch}{\lambda k}\right)^2 \left(\frac{1}{T^2}\right) + \dots} \right]$$

If $\frac{ch}{k} \ll T$, the first term will be small and the second and succeeding terms will be negligible with respect to the first term and may be disregarded. At 10,000 mc, $\lambda = 3$ cm, and $\frac{ch}{\lambda k} = 0.475^\circ\text{K}$. Therefore if the observed temperature is greater than 40 or 50°K all the terms except the first may be safely disregarded. For the problem of interest the temperatures are in the thousands of degrees. Therefore, to a good degree of approximation,

$$\psi_\lambda = \frac{8\pi kT}{\lambda^4}$$

This is known as the Rayleigh-Jeans equation.

The power emitted in a wavelength range $\Delta\lambda$ extending from λ to $\lambda + \Delta\lambda$ by a black body per unit solid angle per unit area of its own surface is given by

$$P_\lambda = \frac{C\psi_\lambda \Delta\lambda}{4\pi} = \frac{2KT}{\lambda^4} c \Delta\lambda$$

Then since $\lambda = \frac{c}{f}$, for small increments $\Delta\lambda = -\frac{1}{c}\lambda^2 \Delta f$ and then

$$P_\lambda = \frac{2kT\Delta f}{\lambda^2}$$

If the source of radiation completely encloses the antenna, and one carries out the integration over the complete solid angle, the total power received is

$$P = kT\Delta f$$

Up to this point black body radiation has been considered. The results can be generalized by using Kirchhoff's radiation law which relates the emission to the absorption properties of a hot body and thus relates the radiated power to its physical state.

Two problems are of general interest; one, is the emission from a body in free space, the other is the emission from a body enclosed in a waveguide. We will be concerned with the latter.

Kirchhoff's radiation law states that if a plane polarized test wave is sent out from the position of the observer and a fraction, A of the incident energy is absorbed by the body, the power, P , emitted in the interval between f and $f + \Delta f$ is related to A by

$$P = kTA\Delta f$$

where

$$A = \frac{\int_{\text{Plasma}} \operatorname{Re} \left(\frac{1}{2} \bar{\mathbf{J}} \cdot \bar{\mathbf{E}} \right) dv}{\int_{\text{Waveguide cross section area}} \operatorname{Re} \left(\frac{1}{2} \bar{\mathbf{E}}_i \times \bar{\mathbf{H}}_i \right) da}$$

A , represents the power absorption coefficient which is defined as the ratio of the power absorbed by a body of volume V to the power incident upon it; \mathbf{J} and \mathbf{E} are the alternating current density and the electric field strength, respectively, at a point within the plasma; and \mathbf{E}_i and \mathbf{H}_i are the unperturbed electric and magnetic-field components of the incident test wave.

If more than one mode propagates down the waveguide within the frequency interval f and $f + \Delta f$, A , represents the sum of the absorption coefficients of the individual modes.

The integration indicated here can be completed but it is still necessary to know the values of the (complex) propagation constant in the section of waveguide containing the plasma and the (complex) plasma conductivity. This would still involve measurements of the plasma characteristics.

Let us examine the definition of A and see whether there is a method of determining A without actually performing the integration.

From the definition, the percentage absorbed power is

$$A = \frac{P_o - P_r - P_t}{P_o}$$

where P_o is the incident power, P_r is the reflected power and P_t is the power transmitted through the plasma.

$$A = 1 - \frac{P_r}{P_o} - \frac{P_t}{P_o} = 1 - \tau_r - \tau_t$$

It is necessary to measure the power reflection and power transmission coefficients τ_r and τ_t . This has been done using the techniques described in II, Microwave Experiments.

It is of interest to know what temperature is actually being measured. The microwave radiation from a volume of ionized gas originates primarily from free-free collisions of electrons with other constituents of the gas. This radiation is referred to as bremsstrahlung. If the electrons have a Maxwellian distribution of velocities

$$h_m(v) = A_1 v e^{-A_2 v^2}$$

then the radiation temperature is the temperature of the electrons.

If the electrons have a Druyvesteyn distribution of velocities

$$h_D(v) = B_1 v e^{-B_2 v^4}$$

the radiation temperature is $0.874 T_e$.

In the cases that have been examined, these temperatures were found to agree approximately with Langmuir probe measurements of the electron temperature.

As far as we know this is the first time that the radiation temperature of a plasma in a "shock-tube" has been measured. The previous measurements have been essentially made on fluorescent tubes mounted in wave guide. Of course, the people in microwave radiometry have long been measuring the radiation temperature of bodies in free space.

In order to measure microwave power, we require a microwave receiver and a device for amplifying the power to a level which can be observed.

The receiver is sensitive to a bandwidth Δf and is tuned to a frequency removed from the local oscillator by the I.F. frequency. This signal is then amplified and detected and averaged.

In general, the receiver also has an image response, i.e., if the signal band is located at $f_{i0} - f_{if}$ the image is at $f_{i0} + f_{if}$.

Let us consider the accuracy of the measurement. Before the plasma appears in the waveguide, we are looking at a load at room temperature and we measure a certain average current with fluctuations at the second detector output. When the hot body appears in the waveguide the average current and the fluctuations both increase. We now want to determine the smallest detectable change in source temperature.

For a square law second detector the average current out is

$$i_{av} = GP_{in}$$

where G is a constant, P_{in} is

$$P_{in} = P_{source} + P_{amp} + P_{Losses}$$

Since the "A" associated with the power due to the losses is very small and the temperature of these losses is about 290°K we can safely neglect this term.

$$P_{\text{source}} = kT_s \Delta f A$$

The noise figure of the amplifier is defined as

$$F = \frac{kT_o \Delta f + P_{\text{amp}}}{kT_o \Delta f}$$

This is the ratio of the noise power at the output of the amplifier to the noise power output which would exist if the amplifiers were noiseless. T_o is defined as 290°K

$$P_{\text{amp}} = (F-1)kT_o \Delta f$$

$$i_{\text{av}} = G \left[KT_s \Delta f A + (F-1) KT_o \Delta f \right]$$

$$i_{\text{av}} = Gk\Delta f \left[T_s A + (F-1) T_o \right]$$

The term $(F-1) T_o$ is often referred to as the noise temperature of the amplifier

$$\Delta i_{\text{av}} = Gk\Delta f \left[\Delta T_s \right] A$$

Now the rms current fluctuations are

$$i_{\text{rms}} = \sqrt{\frac{\Delta f'}{\Delta f}} (i_{\text{av}})$$

where $\Delta f'$ is the bandwidth of the circuit at the second detector output,

then

$$\frac{\Delta i_{av}}{i_{rms}} = \frac{Gk\Delta f(\Delta T_s) A}{\sqrt{\frac{\Delta f'}{\Delta f}} Gk \Delta f [AT_s + (F-1) T_o]}$$

$$\frac{\Delta i_{av}}{i_{rms}} = \frac{\Delta T_s A}{\sqrt{\frac{\Delta f'}{\Delta f}} [AT_s + (F-1) T_o]}$$

If we take $\Delta i_{av} = i_{rms}$, we get

$$\frac{\Delta T_s}{T_s} = \sqrt{\frac{\Delta f'}{\Delta f}} \left[1 + (F-1) \frac{T_o}{AT_s} \right]$$

This gives the percentage change in the source temperature, which would cause the average value of the current to increase by an amount equal to the rms value of the current before the temperature change was made.

Therefore, to see smaller changes in source temperature long integration times, i.e., smaller Δf 's, wide I.F. bandwidths and a low receiver noise figure: must be used. Since the source is broadband noise, the noise figure is 3db less than the single-sideband noise figure since the source puts energy into the image band as well as the normal signal of the receiver of a broadband mixer.

Now suppose we had a $F_{ssb} = 7\text{db}$, $\Delta f' = 1.3 \times 10^5$ cps

$\Delta f = 7 \times 10^6$ cps and $AT_s = 4000^\circ\text{K}$, then

$$\frac{\Delta T_s}{T_s} = 15\%$$

and if the receiver contributed no noise

$$\frac{\Delta T_s}{T_s} = 13.5\%$$

Therefore, to increase the resolution we can increase the I.F. bandwidth, but $\Delta f'$ is determined by the time duration of the plasma in the waveguide.

It is also of interest to compute the ratio of the change in average level to the initial fluctuations for a change in source temperature from T_o to AT_s .

From the previous results

$$(i_{av})_1 = Gk\Delta f \left[T_o + (F-1) T_o \right] = Gk\Delta f F T_o$$

$$(i_{av})_2 = Gk\Delta f \left[AT_s + (F-1) T_o \right]$$

$$\text{Then } \Delta i_{av} = (i_{av})_2 - (i_{av})_1 = Gk\Delta f (AT_s - T_o)$$

$$\text{and } i_{rms} = \sqrt{\frac{\Delta f'}{\Delta f}} (i_{av})_1$$

$$\frac{\Delta i_{av}}{i_{rms}} = \sqrt{\frac{\Delta f}{\Delta f'}} \frac{(AT_s - T_o)}{F T_o}$$

$$= \sqrt{\frac{\Delta f}{\Delta f'}} \left(\frac{1}{F} \right) \left(\frac{AT_s}{T_o} - 1 \right)$$

Let us consider two cases which correspond to actual laboratory experiments.

$$\# 1 \quad \Delta f = 2 \text{ mc}, \Delta f' = 500 \text{ kc}, AT_s = 4000^\circ\text{K}, T_o = 290^\circ\text{K}$$

$$F_{ssb} = 13\text{db}, F = 10\text{db}$$

then

$$\frac{\Delta i_{av}}{i_{rms}} = 2.5$$

$$\#2 \quad \Delta f = 7 \text{ mc}, \Delta f' = 130 \text{ kc}, T_s = 4000^\circ\text{K}, T_o = 290^\circ\text{K}$$

$$F_{ssb} = 7\text{db}, F = 4\text{db}$$

then

$$\frac{\Delta i_{av}}{i_{rms}} = 36$$

One could determine the power gain of the amplifier and work backwards from i_{av} to determine P_{source} and if Δf were known one could finally determine AT_{Source} . This has obvious disadvantages, therefore a standard with a temperature of about $12,000^\circ\text{K}$ is used.

The following Figures are pertinent to this section of the proposal:

Fig. 15. The receiver output as affected by the plasma.

A shift in the signal to noise amplitude begins at about $250 \mu \text{ sec.}$ and lasts for about 100 usec.

Fig. 16. The receiver output as affected by the plasma.

An improved receiver was used. The signal to noise amplitude began to shift at about $300 \mu \text{ sec.}$ and lasted about 200 usec.

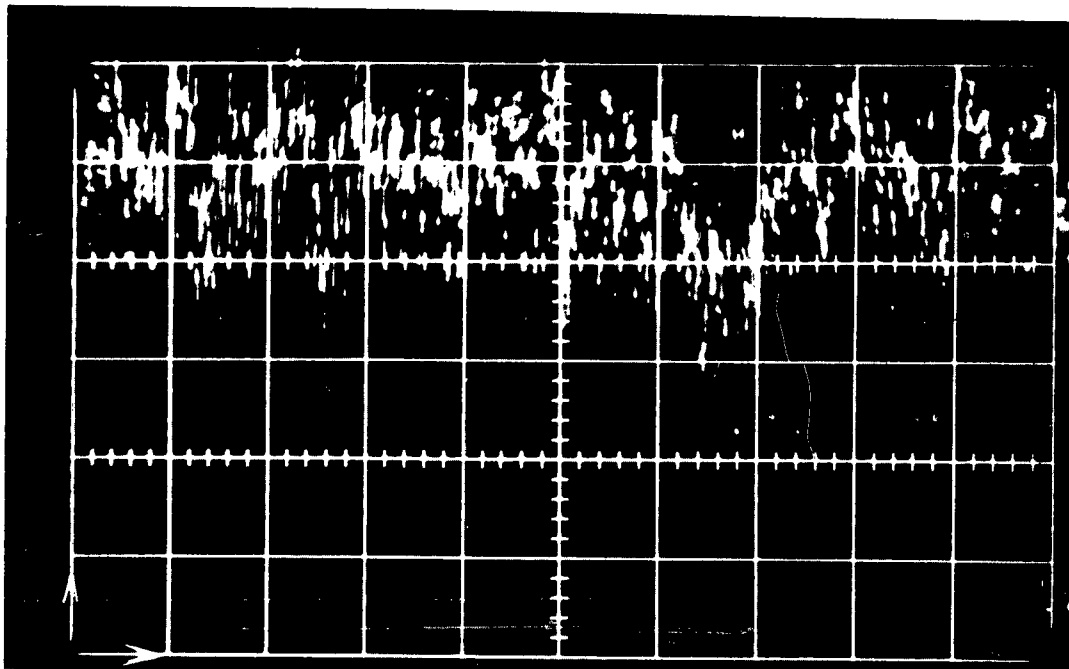


Figure 15. Receiver output as affected by the plasma.
Sweep: $50 \mu\text{sec}/\text{cm}$; $\Delta f = 2\text{mc}$; $\Delta f' = 500\text{kc}$; $T_s \approx 6000^\circ\text{K}$;
 $F = 10\text{db}$.

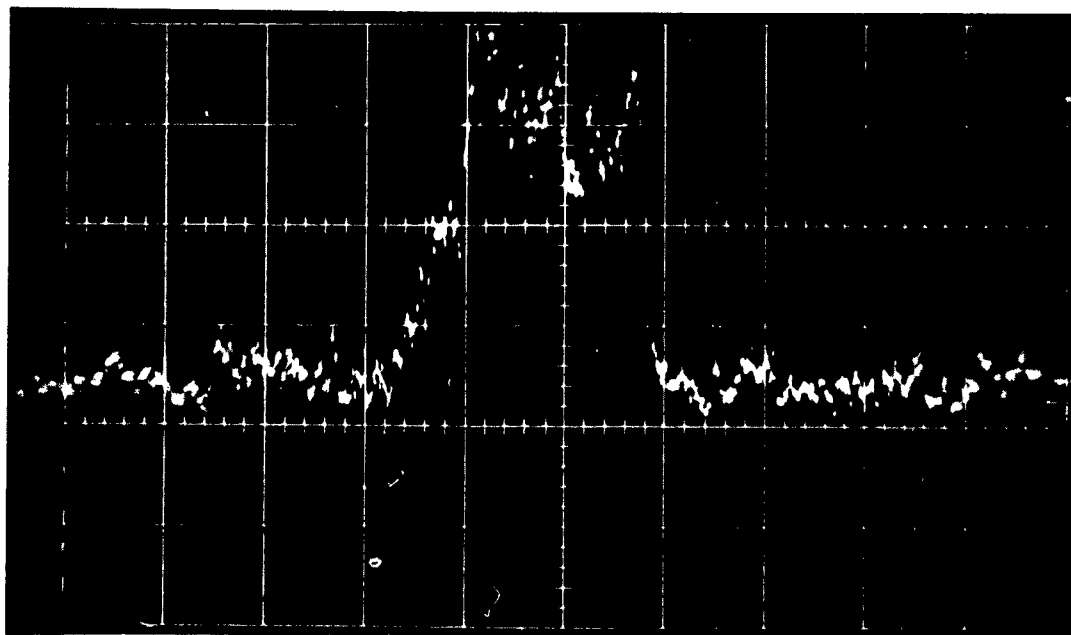


Figure 16. Receiver output as affected by the plasma.
 $100 \mu\text{sec}/\text{cm}$; $\Delta f = 7\text{mc}$; $\Delta f' = 130 \text{kc}$; $T_s \approx 6000^\circ\text{K}$;
 $F = 4\text{db}$.

Fig. 17. System Calibration - The receiver is connected to a temperature reference. A variable microwave attenuator between the receiver and the reference source is used to calibrate the receiver in db.

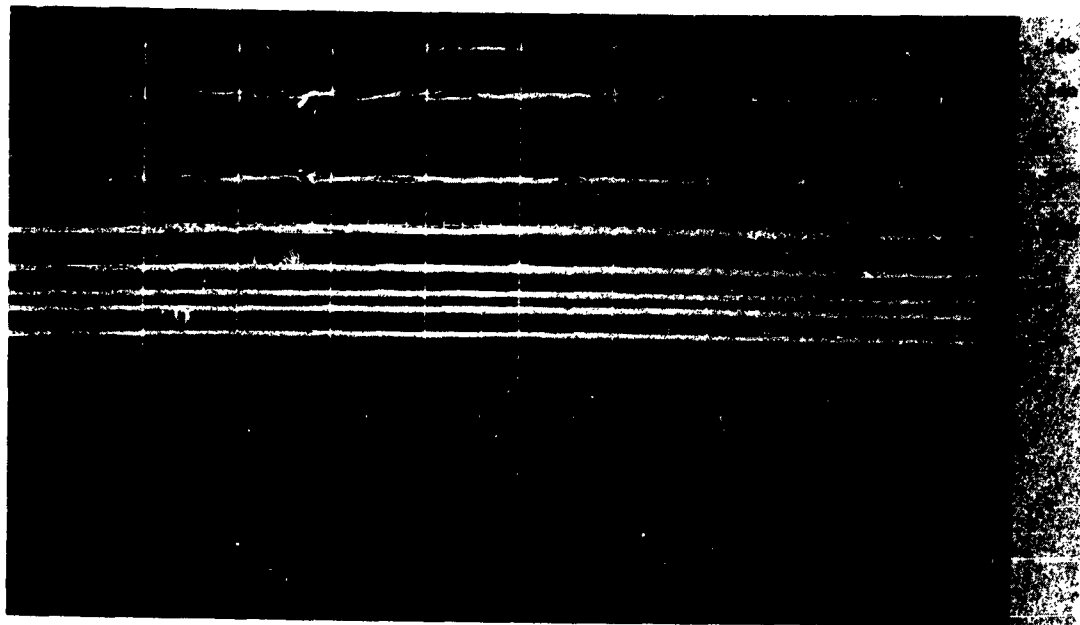


Figure 17. System calibration. Receiver connected to temperature reference with variable microwave attenuator between the receiver and reference source.
Reference temperature = $11,700^{\circ}\text{K}$.

(Figure 2, page 6, shows an assembled view of the shock tube microwave test section.)

VIII Experimental Procedure

Just before the shot, a photograph is taken of the scope deflection for various levels of attenuation between the source and the receiver. As an example, for 3db of attenuation, the equivalent temperature is 6000°K. The receiver is then switched over to the shock tube and the receiver output is recorded on film as the plasma passes through the waveguide test section, after which the receiver is immediately recalibrated.

5. LIST OF EQUIPMENT AND PERSONNEL

Equipment

The following equipment is now in use and it is not anticipated that additional equipment will be required.

1. Completely instrumented DOFL Shock Tube.
2. Microwave radiators, receivers and associated microwave bridge instrumentation.
3. A Mach-Zehnder interferometer with triggered light source and drum camera.
4. Jarrell Asch 75-000 plane grating spectrograph.
5. Beckman-Whitely Model 194 Streak camera.
6. A 400,000 frames per second camera.
7. A Kerr cell camera.
8. The IBM 704 Computer at NBS

Personnel and annual cost for each of 3 programs

Microwave propagation personnel:

			Salary
F. T. Harris	GS-14, Research Supervisor	1/3 time	4000
H. D. Curchack	GS-13, Aeronautical Research Engineer	1/3 time	4000
F. L. Tevelow	GS-12 Physicist	1/2 time	5000
F. J. Nelson	GS-7 Technician	1/3 time	2000
		Overhead	15000
		Total	30000
		Machinist	6000
		Supplies	2000
		Total cost	38000

Stark line broadening personnel:

			Salary
F. T. Harris	GS-14, Research Supervisor	1/3 time	4000
H. D. Curchack	GS-13, Aeronautical Research Engineer	1/3 time	4000
H. Gieske	GS-11, Physicist	Full time	8000
F. J. Nelson	GS-7, Technician	1/3 time	2000
		Overhead	18000
		Total	<u>36000</u>
		Machinist	6000
		Supplies	<u>2000</u>
		Total Cost	44000

Microwave Noise Measurements personnel:

F. T. Harris	GS-14, Research Supervisor	1/3 time	4000
	GS-13, Electronic Engineer	1/2 time	6000
F. L. Tevelow	GS-12, Physicist	1/2 time	5000
H. D. Curchack	GS-13, Aeronautical Research Engineer	1/3 time	4000
F. J. Nelson	GS-7, Technician	1/3 time	2000
		Overhead	21000
		Total	42000
		Machinist	<u>6000</u>
		Total cost	48000

Consultants are:

Dr. F. J. Tischer - Ohio State University

Dr. E. L. Resler, Jr. - Cornell University

Dr. H. Griem assisting H. Gieske on spectroscopy as part of Gieske's thesis at University of Maryland

XI. Background of Personnel

FRED T. HARRIS, GS-14, Physicist, Research Supervisor

Received a bachelors degree with a major in science at Brooklyn College January 1939. Performed graduate work at the University of Maryland majoring in physics, minoring in mathematics from 1948 to 1953. Performed research in fluid dynamics using shock tubes and jets under Doctors Lobb, Bershader and Resler at the Institute for Fluid Dynamics, University of Maryland. AVCO utilized his services in 1955 as a consultant on shock tube work.

From 1956 to present he has been a DOFL research supervisor. He introduced and directed the program covering the effects produced by ionized gases behind strong shock waves. A shock tube and plasma laboratory which contains a heated driver shock tube and two high velocity gas guns were built under his direction.

1953 - 1956, directed work at DOFL involving shock wave effects and phenomena associated with aerodynamic heating.

1950 - 1953 - Naval Medical Research Institute - As physicist conducted blast effects program and participated in atom bomb field tests in Nevada.

1945 - 1950 - Naval Research Laboratory as physicist conducted aeroballistic research using a free flight range. Contributed to the design of an air drag measurement type of ballistic pendulum.

Reports, Articles and Papers Authored or Coauthored

1. A Ballistic Pendulum Air Drag Measurement Technique, Journal of the Aero. Sciences, June 1951.
2. Spark Produced Shock Waves in a Supersonic Wind Tunnel, DOFL Tech Rpt No. TR 149
3. The Shock Tube Facility of DOFL, DOFL Rpt No. 20.1-6R, 8 Dec 1953.
4. Attenuation of a Shock Wave about a 75 MM Projectile, DOFL Rpt. No. 21.5-4R, 30 April 1954.
5. Spark Shock Waves in a Supersonic Wind Tunnel, DOFL Tech. Review Vol. I., October 1957.
6. A Method of Calculating Trajectories, DOFL Rpt. No. TR 422, 15 Jan '57.
7. Shock Tube Generates Waves of Known Intensity, Industrial Laboratories, Feb 1956.
8. Spark Shock Waves - Paper at Army Science Symposium, June 1957.
9. Puff Fuze Feasibility Study, TR 545, Jan 1958.
10. Survey of Anti-Missile Missile Problems, DOFL Internal Rpt R310-59-4.

HERBERT D. CURCHACK, GS-13, Aeronautical Research Engineer

Bachelor of Science in Engineering Physics, New York University, College of Engineering, 1952. Graduate work in Physics and Mathematics at the University of Maryland.

He has been responsible for performing theoretical analysis of a variety of problems in many fields. He has conducted a seminar in The Gas Dynamics at DOFL. He was responsible for the major design of the shock tube, the Mach Zehnder interferometer and associated instrumentation. He designed a finite reservoir wind tunnel which has

specific advantages for measuring specific heat transfer problems.

Mathematical analysis covered magnetostriction, aerodynamic heating, drag deceleration of long range ballistic missiles and gyroscope theory.

Pertinent Reports

1. Balloon for Soft Impact Landing, DOFL Rpt TR-863, 29 August 1960.
2. A simulator for Rapidly Varying Stagnation Conditions, DOFL Rpt R310-60-3, July 1960.

FRANK L. TEVELOW, GS-12, Physicist

He received his Bachelor of Science in Physics from George Washington University in 1956. Since then he has done graduate work at George Washington University and Maryland University.

Prior to working on this project, Mr. Tevelow worked in the field of component testing and electrical measurements. Since January 1959 he has been responsible for the design of the microwave experiment in the shock tube. He has also been primarily responsible for the results obtained to date. Technical reports by Mr. Tevelow on the theory of the measurements and on the experimental techniques are in process.

Pertinent Reports

1. Shock-Tube Microwave Propagation Measurements Using the Dielectric Slab Approximation; F. L. Tevelow and H. D. Curchack; presented at the 2nd Symposium on Engineering Aspects of Magneto-hydrodynamics, sponsored by AIEE, IAS, and IRE at the University of Pennsylvania, 9 & 10 March 1961.

HARRY A. GIESKE, GS-11, Physicist

Educational background:

B. S. (Physics) 1955 - Xavier University, Cincinnati, Ohio
Graduate School (Physics) - University of Maryland
1955 - 1957; 1959 to present

Military Duty - 1957 to 1959

Ordnance Corps, U. S. Army Ordnance
Missile Command, Redstone Arsenal, Ala.
Principal activities were feasibility studies on
proposed missiles and anti-missiles, including missile
design and kill mechanisms.

Civilian Employment - Diamond Ordnance Fuze Laboratories
1955 to 1957; 1959 to present

Principal activities have been in missile trajectory analysis,
aerodynamic heating, and plasma research.

The work proposed here is expected to be used as thesis material
for a Master's degree from the University of Maryland by Mr. Gieske.
His advisor is Dr. Hans Griem.

Dr. Hans Griem is a spectroscopist of considerable note. He is
a member of the faculty of the Physics Department, University of
Maryland and is intimately associated with the AEC-NRL nuclear
fusion program. His most recent work (the Stark line broadening
theory cited in the references) has become a significant tool in the
fusion program.